Experimental study of NIR absorption due to Nb^{4+} polarons in pure and Cr- or Ce-doped SBN crystals

1999 J. Phys.: Condens. Matter 11 4913

(http://iopscience.iop.org/0953-8984/11/25/310)

J. Phys.: Condens. Matter **11** (1999) 4913–4924. Printed in the UK PII: S0953-8984(99)00964-9

Experimental study of NIR absorption due to Nb^{4+} polarons in pure and Cr- or Ce-doped SBN crystals

Ming Gao, S Kapphan, S Porcher and R Pankrath
FB Physik, Universität Osnabrück, 49069 Osnabrück, Germany

Received 15 January 1999, in final form 24 April 1999

Abstract. A broad absorption band around 0.72 eV, assigned to the absorption of Nb^{4+} polarons, is observed in strontium barium niobate (SBN) crystals (nominally pure or Cr- or Ce-doped) either under illumination at low temperature or after a previous reduction treatment. The absorption spectra of Nb^{4+} polarons at low temperature show considerable dichroism, which in reduced SBN crystals exists even far above room temperature. The peak position of the Nb^{4+} polaron absorption in reduced SBN crystals shifts to higher energies with decreasing temperature. The dependence on light intensity and temperature of the Nb^{4+} polaron absorption during the build-up process under illumination and the decay process after the illumination is switched off are investigated in detail. Compared with pure SBN, doping with Ce or Cr creates additional absorption bands in the visible (2.6 eV) and red (1.9 eV for Cr doping) spectral regions. Illumination in these absorption bands at low temperature gives rise to strong Nb^{4+} polaron absorption in the NIR (0.72 eV), giving evidence of the enhanced sensitivity even in the red spectral region for SBN:Cr. The light-induced charge transfer process and formation of Nb^{4+} polarons in SBN are briefly discussed.

1. Introduction

Electron- or hole-polarons are observed in many oxide crystals like TiO_2 [1], MgO [2], $YAlO_3$ [3] $BaTiO_3$ [4, 5] and $LiNbO_3$ [6] by electron spin resonance (ESR) and optical methods. Two methods are usually employed to create polarons in the oxide crystals: suitable irradiation (electron irradiation or illumination) or reduction treatment in vacuum or H_2. The polarons in the oxide crystals show a broad absorption band in the visible or NIR region. Optical investigations of polarons can provide much information about the nature of polarons, such as the polaron energy, the width of the absorption band and its temperature dependence. Polarons are of importance in ferroelectric materials because they play an active role in the light-induced charge transport process. For example, von der Linde and Schirmer found that two-photon photorefractive recording in undoped $LiNbO_3$ crystals is accompanied by an ESR signal of Nb^{4+} polarons and a broad optical absorption band [7]. More recently it was found that the intrinsic polaron contributes to the holographic sensitivity, the refractive index change, light-induced absorption and photoconductivity in $LiNbO_3$:Fe crystals when the crystals are illuminated with high-intensity YAG:Nd laser pulses [8].

Strontium barium niobate $Sr_xBa_{1-x}Nb_2O_6$ (SBN; congruent composition $x = 0.61$) is a photorefractive material presently being considered for a variety of optical applications, such as optical storage [9], data processing [10] and optical phase conjugation [11], because of its high photorefractive sensitivity and large electro-optic coefficient r_{33} [12]. This material belongs to the tetragonal tungsten–bronze family with a partially disordered structure and is known as a relaxor ferroelectric. One unit cell consists of ten NbO_6 linked by their corners in

0953-8984/99/254913+12$19.50

such a way as to form three different types of tunnels A1, A2 and C, along the $\vec{c}$ axis of the crystal. On average, five out of six available A1 and A2 sites are occupied by the cations Sr^{2+} and Ba^{2+} in SBN crystals while C sites are completely empty. Additionally, the composition of SBN can be chosen in a wide range of $0.25 \leqslant x \leqslant 0.75$, which varies the temperature of the diffuse phase transition from the paraelectric phase $4/mmm$ to the ferroelectric phase $4mm$ ($200\,^{\circ}\mathrm{C} \geqslant T_c \geqslant 50\,^{\circ}\mathrm{C}$) [13]. The characteristics of both structure and composition provide great possibilities for SBN to accommodate a wide range of dopants, making it possible to optimize the photorefractive properties of SBN with suitable doping. Ce doping can enhance the photorefractive properties of SBN [12, 14] in the visible and Cr-doped SBN is found to have much faster response speed than other SBN crystals [15, 16]. Furthermore, due to the absorption band of SBN:Cr in the red spectral region, enhanced photorefractive sensitivity in this region is observed in SBN:Cr crystals [17]. However, little is yet known about the origin of the enhanced photorefractive effects in these materials. Light-induced absorption results in SBN:Cr [18] and SBN:Ce [19] demonstrate that a shallow electron trapping centre exists, showing many similarities to Nb^{4+} polarons in $LiNbO_3$:Fe [20]. The Nb^{4+} polaron in SBN was first predicted by Baetzold [21] and experimentally observed in SBN:Ce at low temperature under illumination by an Ar^+ laser (488 nm or 514 nm) or in pure reduced SBN crystals by Greten *et al* [22]. However, the detailed features of Nb^{4+} polarons in SBN crystals have not been investigated so far. This paper reports the results of a study of the properties of light-induced Nb^{4+} polarons in SBN:Cr and SBN:Ce crystals. The absorption dichroism, the dependence on illumination intensity and on temperature and the build-up and decay processes when the illumination is switched on and off are presented. For comparison, results obtained from reduced SBN crystals, with respect to the Nb^{4+} polaron absorption, are also discussed.

2. Experimental techniques

The absorption measurements were performed with a high-resolution Fourier Spectrometer (up to 10^{-3} cm^{-1}, Bruker IFS120 HR) using photomultiplier and GaP/Si diodes for the UV–VIS region, and LN_2-cooled Ge, InSb or HgCdTe detectors for the NIR–FIR range. Pure and doped congruent $Sr_{0.61}Ba_{0.39}Nb_2O_6$ crystals with different amounts of Ce or Cr in the melt were grown by the Czochralski method in the crystal growth laboratory of the University of Osnabrück. The crystals were cut parallel or perpendicular to the ferroelectric $\vec{c}$ axis and poled under an applied electric field (>10 kV cm^{-1}) at $T = 70\,^{\circ}\mathrm{C}$ (the temperature for the diffuse phase transition in congruent undoped SBN is about $80\,^{\circ}\mathrm{C}$). An Ar^+ laser or a Kr^+ laser (Spectra Physics, Model 171, 488 nm, 514 nm and 647 nm) or a xenon lamp (ILC Cermax, 150 W) with a dichroic filter ($\lambda < 500$ nm reflected and $\lambda > 500$ nm transmitted) were used as illumination sources for the light-induced absorption measurements. Scattered laser light in the probe light beam was removed with holographic notch filters. For some measurements the samples were placed in a bath cryostat under immersion conditions in superfluid helium or LN_2 (77 K) to ensure stable temperature conditions even under strong illumination. The reduction treatment was performed in an Ar or vacuum atmosphere at $T = 1000\,^{\circ}\mathrm{C}$.

3. Experimental results

The absorption spectra of SBN:Cr, SBN:Ce and pure SBN crystals at room temperature are shown in figure 1. The SBN:Cr crystal has broad absorption bands around 1.9 eV (650 nm)

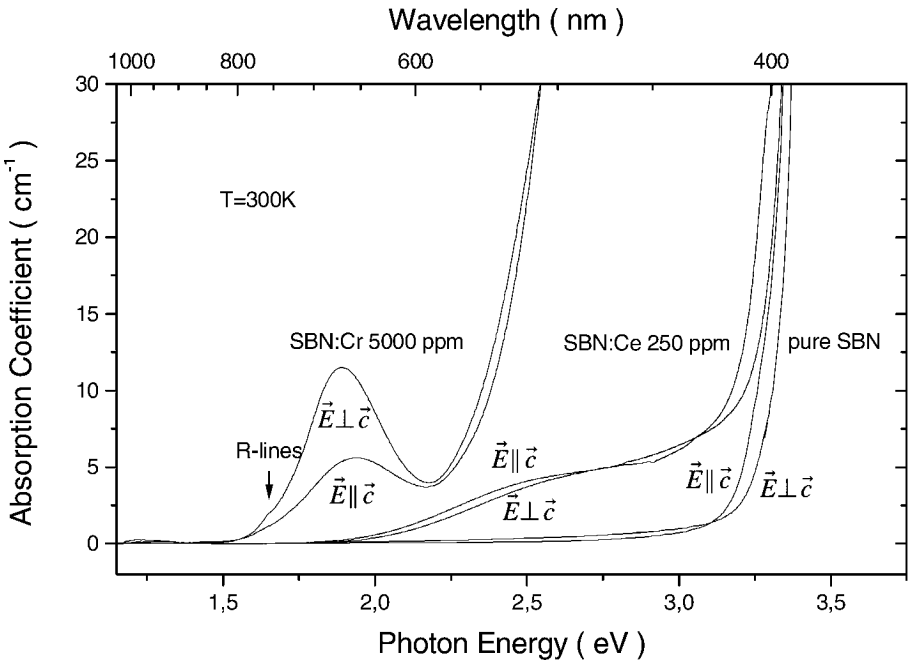

Figure 1. Polarized absorption spectra in congruent pure SBN, SBN:Ce (0.025 wt% Ce in the melt) and SBN:Cr (5000 ppm Cr in the melt) at room temperature. $\vec{E}$ denotes the vector of the probe light and the $\vec{c}$ the axis of the crystals.

and around 2.6 eV (475 nm), which show a considerable dichroism and are very similar to the characteristic absorption bands of Cr^{3+} in $LiNbO_3$:Cr [23] and other Cr-doped oxide crystals [24]. The appearance of R-lines in absorption at 1.65 eV (750 nm), broadened by the structural disorder, confirms the existence of Cr^{3+} in SBN:Cr. Actually x-ray photoelectron spectroscopy (XPS) experiments of SBN:Cr and SBN:Ce demonstrate that Cr^{3+} and Ce^{3+} are the dominant charge states of Cr and Ce ions in SBN [25]†. Other experimental evidence for Ce^{3+} in SBN crystals comes from FIR absorption [26, 27], ESR [28] and photoconductivity [29] measurements. Instrumental neutron activation analysis of SBN:Ce and SBN:Cr shows that Ce ions occupy Sr/Ba sites and Cr ions are located in Nb sites [30]. The absorption spectra of SBN:Ce show a wide dichroic shoulder extending from band edge to 2 eV. In the NIR and MIR spectral regions no other absorption bands are observed, except for the weak vibration absorption band of OH around 3500 cm^{-1}, in SBN:Cr and SBN:Ce crystals [26]. In the FIR region the lattice vibration absorption appears at about 2000 cm^{-1} in SBN crystals, with additional absorption in SBN:Ce due to the spin-orbit and crystal field split levels of the 4f electron of Ce^{3+} [27].

Under illumination with a Kr^+ laser (647 nm; photon energy, 1.92 eV) at low temperature, SBN:Cr shows a broad polaron absorption with an intensity of several orders of magnitude higher than that of SBN:Ce under the same conditions, as shown in figure 2. The photon energy (1.92 eV) of the laser just lies inside the first absorption band of SBN:Cr and outside the absorption shoulder of SBN:Ce. One important conclusion can be drawn here. Cr^{3+} indeed behaves as the electron donor in the light-induced charge transport process of SBN:Cr at low temperature since the majority of light-induced charge carriers are electrons [31, 32]. In fact,

† XPS experiment of SBN:Cr showed that more than 90% of Cr is in Cr^{3+} state (M Neumann, private communication).

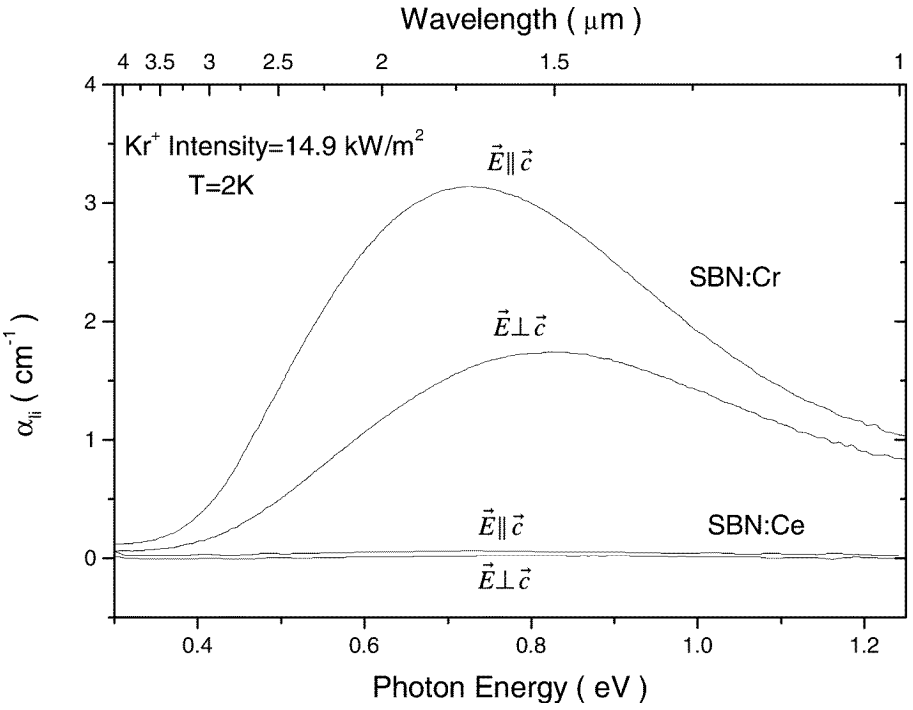

Figure 2. The light-induced polaron absorption band under polarized probe light in SBN:Cr (500 ppm Cr in the melt) and SBN:Ce (0.025 wt% Ce in the melt) crystals at 2 K. A Kr^+ laser (647 nm) was employed as the illumination source.

if we illuminate the SBN:Ce crystal with an Ar^+ laser (488 nm and 514 nm; photon energy, 2.55 eV and 2.42 eV, lying within the absorption shoulder of SBN:Ce) at low temperature, we do observe a polaron absorption band similar to that in SBN:Cr. A pure SBN crystal does not show this polaron absorption band under illumination with an Ar^+ laser or a Kr^+ laser, but the Nb^{4+} polarons can be created by illumination with UV light in the band edge region. A similar polaron absorption band was also observed in $LiNbO_3$ under illumination at low temperature or after a reduction treatment and could be assigned to Nb^{4+} polaron absorption from ESR measurements [6, 33, 34] and theoretical treatments [38, 39]. Laser beam coupling experiments have shown that SBN:Cr crystals have an enhanced photorefractive sensitivity in the red spectral region as compared to SBN:Ce crystals [16, 17]. From observations of the light-induced polaron absorption, SBN:Cr also shows an enhanced sensitivity in the red due to the extended absorption band in the red spectral region. Both Cr and Ce dopings enhance the response sensitivity of SBN crystals in the visible spectral region.

Considerable dichroism is observed for the Nb^{4+} polaron absorption band at 1.6 μm. At 2 K, the light-induced absorption shows a ratio $\alpha_{li}(\vec{E}_L \| \vec{c})/\alpha_{li}(\vec{E}_L \perp \vec{c}) \approx 2$, and the peak positions vary slightly for the two components (0.72 eV for the parallel component and 0.78 eV for the perpendicular component). According to small polaron theory, the binding energy of Nb^{4+} polaron in SBN crystals is about 0.36–0.39 eV and the thermal hopping energy is about 0.18–0.19 eV [35].

At 2 K under immersion in superfluid helium, the illumination intensity dependence of the Nb^{4+} polaron absorption is shown in figure 3.

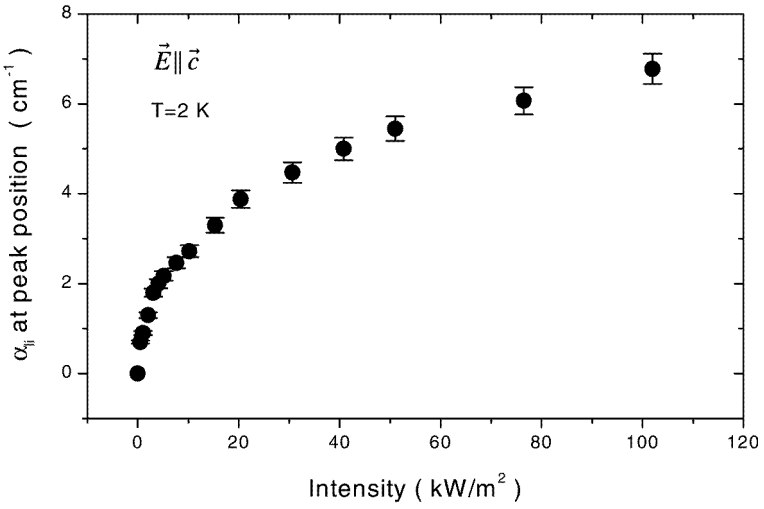

Figure 3. Illumination intensity dependence of the polaron absorption in SBN:Cr (500 ppm Cr in the melt) at 2 K (immersion technique). A Kr^+ laser (647 nm) was used as the illumination source.

According to Smakula's formula:

$$\alpha_{li} w = A n_p f \tag{1}$$

or

$$\alpha_{li} = \frac{Af}{w} n_p \tag{2}$$

where α_{li} is the absorption coefficient at the peak position, n_p is the concentration of polarons, A is a constant, w is the full width at half maximum of the absorption band and f is the oscillator strength of the optical transition. At one fixed temperature, the oscillator strength f and the full band width w in the above equations are constants, which means $\alpha_{li} \propto n_p$. The dependence of α_{li} on the illumination intensity clearly tends to show a square-root-like behaviour, as shown in figure 3.

The peak position and the full band width at half maximum of the absorption band vary little with the temperature for $T < 130$ K, as shown in figure 4. The temperature dependence of α_{li} under constant illumination intensity in pure SBN, SBN:Cr and SBN:Ce is demonstrated in figure 5. Below 70 K, α_{li} for a constant illumination intensity changes very little with temperature, indicating that n_p is actually a constant at low temperature if the oscillator strength of the optical transition does not change much with temperature, which can be inferred from the weak temperature dependence of the integral Nb^{4+} polaron absorption in reduced SBN crystals [22]. Nb^{4+} polaron absorption in reduced SBN crystals, being visible far above room temperature, is shown in figure 6. The reduced SBN crystal shows a broad NIR absorption band whose peak is located at 0.72 eV and 0.78 eV for the parallel ($\vec{E} \| \vec{c}$ axis) and perpendicular ($\vec{E} \perp \vec{c}$ axis) components respectively. A similar Nb^{4+} polaron absorption band has also been documented in reduced $LiNbO_3$ crystals [33] and identified by ESR experiments to belong to Nb^{4+} [34]. No other absorption band due to the reduction treatment was observed in this reduced crystal.

The tendency of light-induced Nb^{4+} polaron absorption α_{li} in the steady state under a constant illumination intensity to slowly decrease at low temperature can be interpreted as due to a small variation of the oscillator strength in this low temperature range. Above 70 K

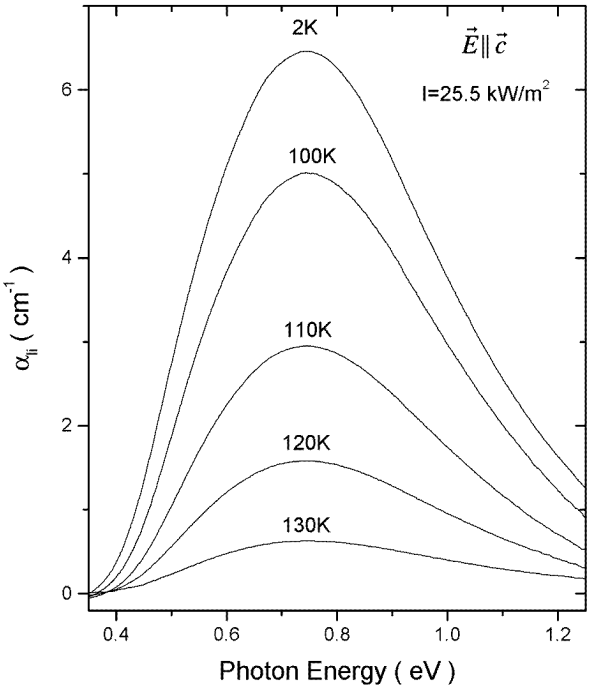

Figure 4. Polaron absorption bands in SBN:Cr (500 ppm Cr in the melt) at different temperatures. An Ar^+ laser (488 nm, 25.5 kW m^{-2}) was used as the illumination source.

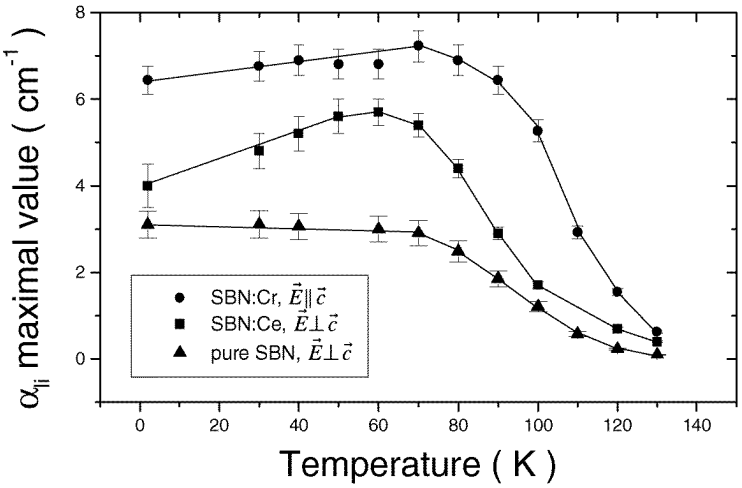

Figure 5. Temperature dependence of the polaron absorption in pure SBN, SBN:Cr (500 ppm Cr in the melt) and SBN:Ce (0.025 wt% Ce in the melt). An Ar^+ laser (488 nm) was used as the illumination source in the light-induced absorption measurements in SBN:Cr and SBN:Ce ($I = 25.5$ kW m^{-2}), and a xenon lamp with a dichroic filter ($\lambda < 500$ nm, approximately 20 kW m^{-2}) was used as the illumination source in the case of the pure SBN crystal. The full curves are guides for the eye.

α_{li} decreases more and more rapidly with increasing temperature and it actually becomes undetectable above 140 K under the present experimental conditions.

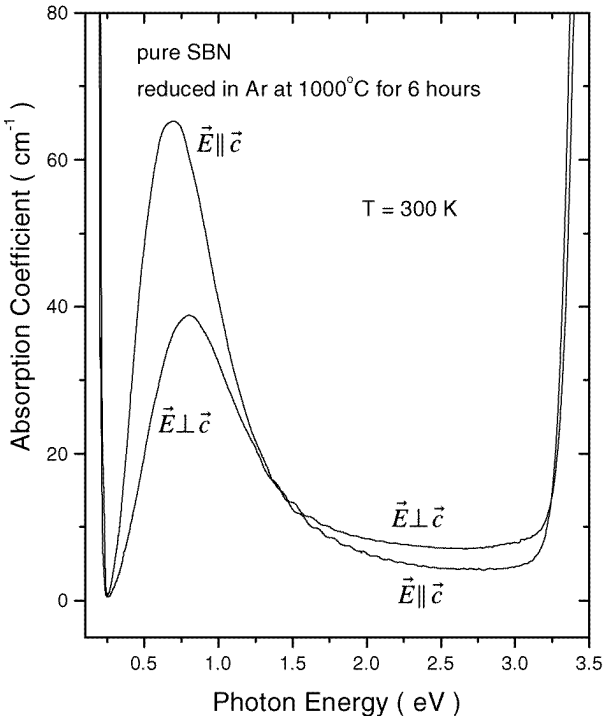

Figure 6. The polarized absorption spectra of a pure SBN crystal at room temperature after the crystal had been reduced in Ar at 1000 °C for 6 h.

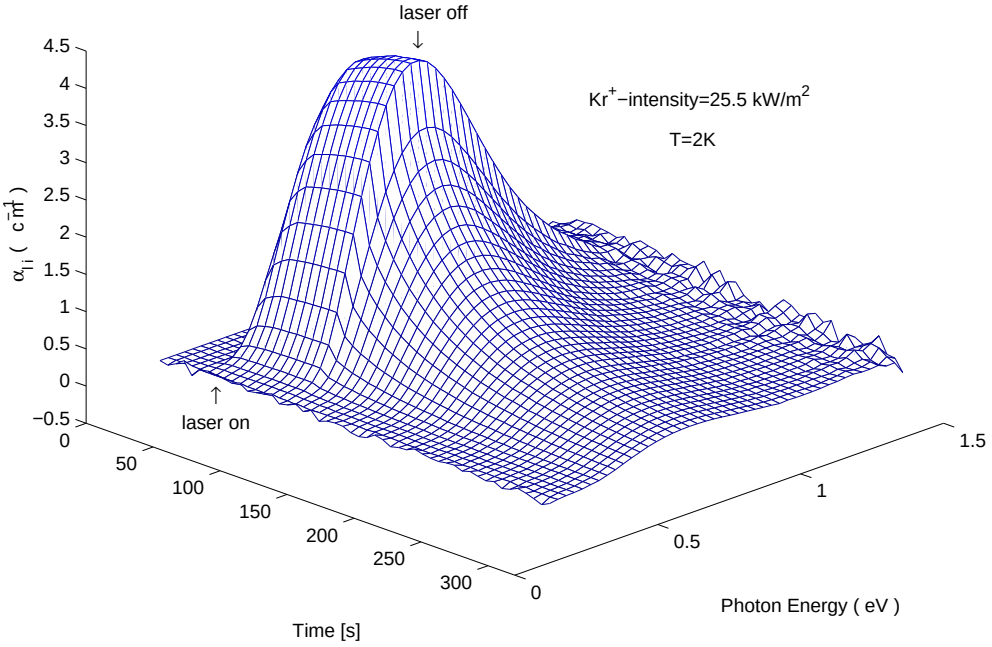

Figure 7. 3D build-up and decay of polaron absorption in SBN:Cr (500 ppm Cr in the melt) after the Kr^+ laser (647 nm, 25.5 kW m^{-2}) illumination was switched on and off.

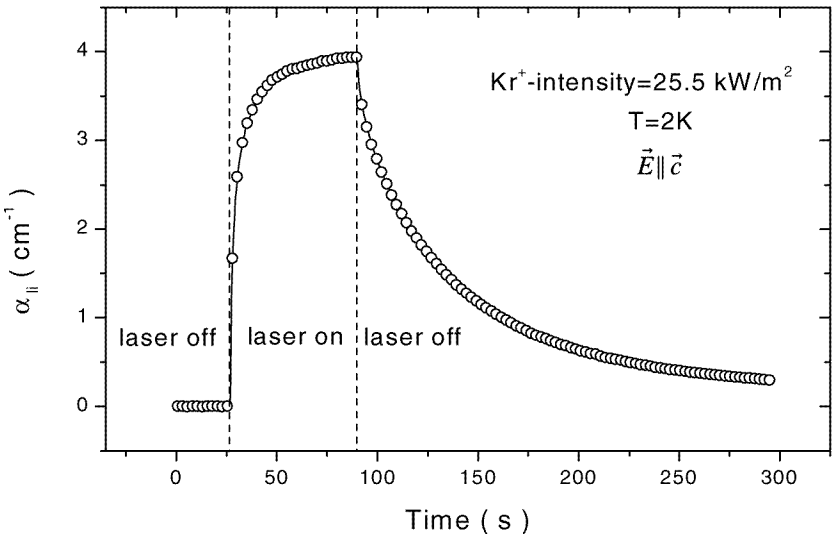

Figure 8. The build-up and decay at 2 K of polaron absorption at the peak position (0.72 eV) in SBN:Cr (500 ppm Cr in the melt) after the Kr^+ laser (647 nm, 25.5 kW m^{-2}) was switched on and off.

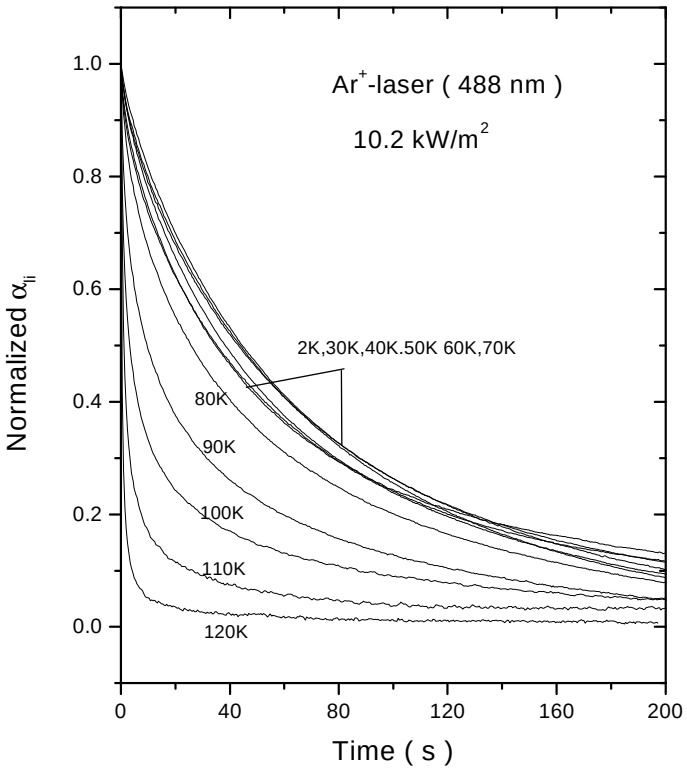

Figure 9. The temperature dependence of the normalized decay process of the light-induced polarons in SBN:Cr (500 ppm Cr in the melt). An Ar^+ laser (488 nm, 10.2 kW m^{-2}) was used as the illumination source.

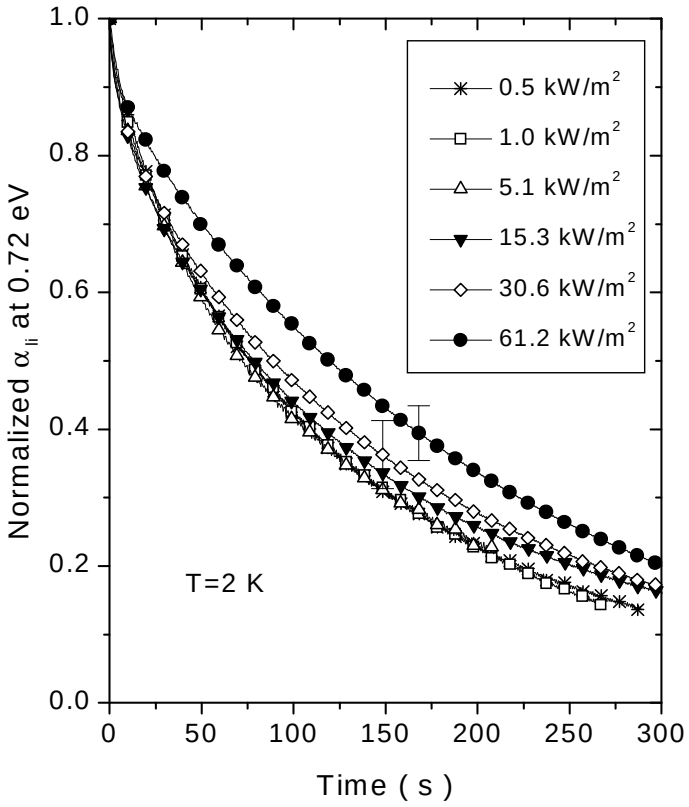

Figure 10. The normalized decay process of light-induced polarons in SBN:Cr (500 ppm Cr in the melt) after switching off laser illumination of different intensities at 2 K (immersion technique). An Ar^+ laser (488 nm) was used as the illumination source.

The build-up and decay processes of polaron absorption under switched illumination are shown in figure 7 as a 3D plot and figure 8 as a contour plot of the time dependence of the maximum α_{li}. The decay process of polaron absorption is found to be non-monoexponential after the laser is switched off. It was formerly fitted with the addition of two exponents but no physical meaning was given for such a fitting [22]. Recently a model to describe the light-induced charge transport process in doped SBN crystals was developed to explain the dynamics of the light-induced Nb^{4+} polaron, the details of which will be published elsewhere [37]. Figure 9 shows the normalized decay curves of polaron absorption at different temperatures after the removal of illumination. Below 80 K the decay process of the light-induced Nb^{4+} polaron absorption is nearly temperature independent, which indicates that a temperature-independent decay channel plays a major role here. However, the decay process becomes faster with temperatures above 80 K, indicating that here a thermally activated decay channel begins to dominate the decay process. The decay process of the Nb^{4+} polarons is found to depend not very strongly on the illumination intensity or, correspondingly, on the starting concentration of Nb^{4+} polarons. Figure 10 shows the decay processes of the Nb^{4+} polarons after removal of laser illumination of different intensities. For a variation of the illumination intensity of more than two orders of magnitude the $1/e$ point varies only by a factor of about two (from 120 s to 181 s).

4. Discussion and conclusion

SBN crystals belong to the class of oxygen-octahedra ferroelectric crystals. The highest filled valence band in niobate crystals [21, 36] is based on oxygen 2pπ orbitals, which interact through ligand–metal π bonding with the dϵ orbitals of Nb^{5+}. The conduction band is based on the dϵ orbitals of Nb^{5+}, which are empty in a perfect crystal. The interband transition of SBN crystals comes from the electron transition from 2pπ orbitals of oxygen to the dϵ orbitals of Nb^{5+} ions and the bandgap is about 3.36 eV (370 nm). The absorption spectra of SBN:Ce crystals show that the ground state of Ce^{3+} centres falls in the bandgap of the SBN crystal and the first excited state of Ce^{3+} lies close to or higher than the bottom of the conduction band. Under illumination of suitable wavelength an intervalence transition 4f (Ce^{3+}) $\rightarrow$ 4d (Nb^{5+}) occurs. The 1.9 eV absorption band of SBN:Cr crystals originates from the 3d intershell transition of Cr^{3+}. However, when one electron is excited by red light (647 nm) from the ground state of Cr^{3+} to the first excited state, this state should be situated shallow below the conduction band edge. The electron in the excited state can be further excited to the conduction band (dϵ orbitals of Nb^{5+}) with the absorption of another photon or phonons. In this way photoionization of Cr^{3+} occurs and results in the generation of electrons in the conduction band. The electrons in the conduction band can be trapped by their self-induced potential well by electron–lattice coupling interactions and form Nb^{4+} polarons. The illumination of pure SBN crystals with Ar^{+} or Kr^{+} lasers (488 nm, 514 nm or 647 nm) cannot create an observable number of Nb^{4+} polarons because the photon energy is not sufficient to excite an electron from the valence band to the conduction band. However, illumination with UV light at low temperature indeed generates Nb^{4+} polarons in pure SBN crystals as shown in figure 5.

One important point which should be noted is that most Nb^{4+} polarons are probably formed close to those Ce^{4+} or Cr^{4+} or O^{-} where the electrons originated from. In other words, electrons photoexcited from Ce^{3+} or Cr^{3+} or O^{2-} to Nb^{5+} ions will be trapped, resulting in nearby Nb^{4+} polarons at low temperature. The electrons trapped in Nb^{4+} polarons can transit the potential barrier between Nb^{4+} polarons and $Ce^{4+}/Cr^{4+}/O^{-}$ ions by direct tunnelling, phonon-assisted tunnelling, or over the barrier transition. At superfluid helium temperature (2 K), thermal over the barrier transitions of electrons in the Nb^{4+} polarons are frozen out and only the tunnelling processes contribute to the decay process. The probability of the tunnelling process decreases rapidly with increasing distance. The decay process of light-induced Nb^{4+} polaron absorption after the illumination is switched off closely follows a description due to only next nearest neighbour Nb^{4+} polarons [37]. The tunnelling process is also reflected by the temperature-independent decay process of Nb^{4+} polarons from 2 K to 70 K (see figure 9). Above 70 K a thermally activated over the barrier transition and the hopping motion between different Nb^{4+} sites tend to contribute to the decay process and therefore a faster decay process with increasing temperature is observed.

The strength of the electron–lattice interaction controls the probability of electrons in the conduction band forming Nb^{4+} small polarons during illumination. For a sufficiently weak electron–lattice interaction a small polaron state is unstable and only the Bloch state of electrons in the conduction band occurs. The presence of electrons induces only minimal changes in the positions of surrounding atoms. If the interaction is very strong, for example, in soft and deformable crystals, the electron in a Bloch state is dynamically unstable and it will be trapped as a Nb^{4+} small polaron. The formation of small polarons causes a substantial displacement of the surrounding atoms. The polaronic state and the usual conduction band state can coexist in the case of a moderate electron–lattice coupling strength. Although the absorption of Nb^{4+} polarons in SBN crystals is very pronounced, it is difficult to detect by EPR

techniques. A possible reason for the absence of the EPR signal could be seen in a very fast spin-lattice relaxation [38].

In conclusion, we can state that at low temperature an optical NIR absorption band due to Nb^{4+} polarons can be observed both in SBN crystals under illumination as well as in reduced SBN crystals. Above 130 K the Nb^{4+} polarons found in the reduction treatment remain stable and can be observed at elevated temperatures well above room temperature. In contrast to this behaviour, the light-induced Nb^{4+} polarons show a fast decay above 130 K and are no longer observable under the present experimental conditions at higher temperatures. Cr and Ce doping expands the spectral response of SBN crystals to the visible region and Cr doping in particular enhances the response sensitivity in the red in comparison with Ce doping. A nonlinear illumination intensity dependence of the light-induced Nb^{4+} polaron absorption is observed. At $T < 80$ K, the temperature-independent tunnelling process can be assumed to play a dominant role in the decay process of the light-induced Nb^{4+} polarons and at $T > 80$ K the temperature-dependent hopping motion of the polarons begins to dominate the decay process. Many details of the decay process of light-induced polarons, such as the weak dependence on the starting concentration of polarons, are not fully understood at present and further theoretical and experimental investigations are needed.

Acknowledgments

This work is supported by DFG (SFB225, C7). We thank Professor Dr O F Schirmer for valuable comments and suggestions. One of the authors (Ming Gao) is grateful for a doctoral fellowship of the VW Foundation.

References

[1] Bogomolov V and Mirlin D 1968 *Phys. Status Solidi* **27** 443
[2] Chen Y and Sibley W A 1967 *Phys. Rev.* **154** 842
[3] Schirmer O F, Blazey K W and Berlinger W 1975 *Phys. Rev.* B **11** 4201
[4] Mazur A, Schirmer O F and Mendricks S 1997 *Appl. Phys. Lett.* **70** 2395
[5] Scharfschwerdt R, Mazur A, Schirmer O F and Mendricks S 1996 *Phys. Rev.* B **54** 15 284
[6] Schirmer O F and von der Linde D 1978 *Appl. Phys. Lett.* **33** 35
[7] von der Linde D and Schirmer O F 1978 *Appl. Phys.* **15** 153
[8] Simon M, Jermann F and Krätzig E 1995 *Appl. Phys.* B **61** 89
[9] Ford J E, Ma J and Fainman Y 1992 *J. Opt. Soc. Am.* A **9** 1183
[10] Yeh P and Chiou A E T 1987 *Opt. Lett.* **12** 138
[11] Wood G L, Clark III W W, Miller M J, Sharp E J, Salamo G J and Neurgaonkar R R 1987 *IEEE J. Quant. Electron.* **23** 2126
[12] Neurgaonkar R R, Cory W K, Oliver J R, Ewbank M D and Hall W F 1987 *Opt. Eng.* **26** 392
[13] Ballman A A and Brown H 1967 *J. Crystal Growth* **1** 311
[14] Megumi K, Kozuka H, Kobayashi M and Furuhata Y 1977 *Appl. Phys. Lett.* **30** 631
[15] Vazquez R A, Ewbank M D and Neurgaonkar R R 1991 *Opt. Commun.* **80** 253
[16] Sayano K, Yariv A and Neurgaonkar R R 1989 *Appl. Phys. Lett.* **55** 328
[17] Tomita Y and Suzuki A 1994 *Appl. Phys.* A **59** 579
[18] Orlov S, Segev M, Yariv A and Neurgaonkar R R 1994 *Opt. Lett.* **19** 1293
[19] Simon M, Gerwens A and Krätzig E 1994 *Phys. Status Solidi* a **143** K125
[20] Simon M, Jermann F and Krätzig E 1994 *Opt. Mater.* **3** 243
[21] Baetzold R 1993 *Phys. Rev.* B **48** 5789
[22] Greten G, Kapphan S and Pankrath R 1995 *Rad. Eff. Def. Solids* **135** 195
[23] Fischer C, Kapphan S, Xi-Qi Feng and Ning Cheng 1995 *Rad. Eff. Def. Solids* **135** 199
[24] Wood D L, Ferguson J, Knox K and Dillon J F Jr 1963 *J. Chem. Phys.* **39** 890
[25] Niemann R, Buse K, Pankrath R and Neumann M 1996 *Solid State Commun.* **98** 209
[26] Hunsche S, Gröne A, Greten G, Kapphan S, Pankrath R and Seglins J 1995 *Phys. Status Solidi* a **148** 629

[27] Greten G, Hunsche S, Knüpffer U, Pankrath R, Siefker U, Wittler N and Kapphan S 1996 *Ferroelectrics* **185** 289
[28] Giles N C, Wolford J L, Edwards G L and Uhrin R 1995 *J. Appl. Phys.* **77** 976
[29] Simon M, Buse K, Pankrath R and Krätzig E 1996 *J. Appl. Phys.* **80** 251
[30] Woike Th, Weckwerth G, Palme H and Pankrath R 1997 *Solid State Commun.* **102** 743
[31] Greten G 1996 *PhD Thesis* University of Osnabrück
[32] Ewbank M D, Neurgaonkar R, Cory W K and Feinberg J 1987 *J. Appl. Phys.* **62** 374
[33] Arizmendi L, Cabrera J M and Agulló-López F 1984 *J. Phys. C: Solid State Phys.* **17** 515
[34] Schirmer O F, Thiemann O and Wöhlecke M 1991 *J. Phys. Chem. Solids* **52** 185
[35] Faust B, Müller H and Schirmer O F 1994 *Ferroelectrics* **153** 297
[36] Clark M G, DiSalvo F J, Glass A M and Peterson G E 1973 *J. Chem. Phys.* **59** 6209
[37] Gao M, Pankrath R, Kapphan S and Vikhnin V 1999 *Appl. Phys.* B **68** 849
[38] Deleo G G, Dobson J L, Masters M F and Bonjack L H 1998 *Phys. Rev.* B **37** 8394
[39] Hafid C and Michel-Calendini F M 1986 *J. Phys. C: Solid State Phys.* **19** 2907